



FEEDFORWARD ALGORITHMS WITH SIMPLIFIED PLANT MODEL FOR ACTIVE NOISE CONTROL

M. PAWEŁCZYK

Institute of Automatic Control, Silesian University of Technology, ul. Akademicka 16, 44-101 Gliwice, Poland. E-mail: mpawelczyk@ia.polsl.gliwice.pl

(Received 21 March 2000, and in final form 26 October 2001)

Most feedforward active noise control (ANC) algorithms require models of electro-acoustic paths. To obtain satisfactory attenuation and keep the system stable these models have to represent the plant well. This, according to the literature, requires estimation of many, often hundreds of coefficients. Then, control filters also have very large, comparable structures. Such an approach reveals significant drawbacks if paths of the plant are subject to change. Estimation of so many plant models and control filter coefficients is very slow and time consuming. Therefore, the speed of adaptation is substantially reduced. This can be accepted in some unmoveable plants like acoustic ducts. However, there are many other plants, e.g., active personal hearing protection devices, in which rapid reaction is also of utmost interest not to annoy the user. In this paper, an alternative approach is proposed that does not need precise models except an estimate of the discrete time delay of the plant. However, according to the literature this leads to a relatively narrow attenuation band, which is confirmed for classical control structures like finite and infinite impulse response filters. This becomes a premise to design a new control algorithm. First, the so-called phase shifters (in two versions) are designed. They enable to control narrowband noise on comparable levels with at least an order less parameters than the filters mentioned above. To control broadband noise, the idea of phase shifter banks is then put forward. In turn, to extend the attenuation band conversion of sampling frequency is adopted to noise control problems. Finally, the algorithm combining advantages of phase shifter banks and conversion of sampling frequency allows controlling of any noise over any frequency band, with limits imposed only by the signal processor available and pass-band of the secondary source. Although this algorithm is designed generally and can be applied to any ANC plant, for laboratory experiments an active personal hearing protection device is used.

© 2002 Elsevier Science Ltd. All rights reserved.

1. INTRODUCTION

In this paper a feedforward digital control system, as generally presented in Figure 1, is considered. A signal from the reference microphone filtered by a feedforward controller drives the secondary source. A signal from the error microphone is used to supervise updating of the controller parameters. Although ANC systems, in general, are taken into account and the entire algorithm designed in this paper can be successfully applied to any of them, particular emphasis is placed on compact acoustic plants (CAP) [1]. For such plants, due to geometrical arrangement of the system components, with digital control and a given sampling rate and set-up, processing times of electric signals from both reference and error microphones to the secondary source (sources, in general) are longer than propagation times of acoustic waves between points in which these components are placed. For example, it is impossible to detect the primary noise by the reference microphone, transform it into an

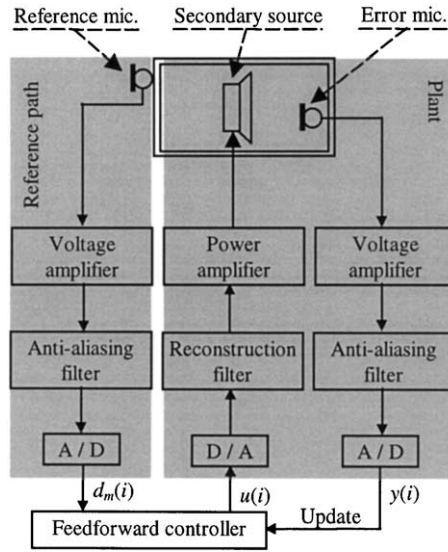


Figure 1. Feedforward active noise control system.

electrical signal, process it, produce the control signal, transform it into the secondary sound and send it to the area of interest before the primary noise reaches it. Therefore, CAPs are said to require non-causal actions (see, e.g., reference [2]). Active personal hearing protection devices (APHPD) with reference microphones mounted on the external sides of the earmuffs are representatives of such plants (other examples of CAPs are active headrests, “silent lamps”, etc.). Although the vast majority of APHPDs is still based on analogue feedback controllers [3], during recent years several research groups have been working on the application of adaptive digital control techniques to such devices in order to obtain better performance. Some authors employ reference sensors (in feedforward digital algorithms) placed near the primary source (far from the device) if the noise is periodic and the APHPD is designed as “unmoveable”. The reference sensors are, for example, tachometers collecting signals from rotors in aircraft [4], or other rotating machinery like car engines and toothed wheels [5], or accelerometers measuring vibration of the noise generator. However, any noise originating from other sources is not attenuated then. Therefore, some researchers try to combine digital feedforward algorithms with feedback (usually analogue) algorithms [6].

In this paper, feedforward control will be considered. However, contrary to most designs given in the literature a simplified plant model, i.e., only its discrete time delay, will be employed. Such an approach allows the getting rid of the time-consuming estimation of large plant and consequently control filter structures, thereby significantly speeding up the processing and reducing sensitivity of the control algorithm to plant parameters fluctuation. Adequate control filters are proposed. In the remainder they are combined in filter banks controlling broadband noise, and further—in multirate structures extending the attenuation band. The computational burden is analyzed and many experimental results are provided proving the thesis that the proposed algorithm allows effective control of any sound over any band (with limitation only due to the speed of the signal processor) with very fast convergence, which taken together gives acoustic comfort to the user.

2. THE ADAPTIVE CONTROL SYSTEM

All the experiments presented in this paper will be performed on the APHPD constructed by the author. This device consists of a passive personal hearing protection device equipped with two omnidirectional electret microphones and a small loudspeaker. For experiments, to ensure the same working conditions and avoid listening to very high-level unpleasant noise, the earmuff is applied to an artificial head, which mimics the acoustic properties of the human ear. Both the head and the headset itself, of course, terminate the cavity where the controlled noise propagates. The artificial head contains an observer microphone to monitor attenuation results; it is not employed by control algorithms. Both the anti-aliasing and reconstruction filters used in this work (see Figure 1) are fourth order Butterworth filters and have their cut-off frequencies set at 650 Hz, which guarantees attenuation at the Nyquist frequency (1 kHz) of about 10 dB, each. All control algorithms considered in this paper are feedforward digital algorithms implemented on DS1102 board with TMS320C31 floating point signal processor.

Magnitudes and phases of frequency responses of the plant (see Figure 1) with various loads are presented in Figures 2 and 3 respectively. As it is seen, provided the earmuff is tightly sealed (but not annoyingly), the responses for the artificial and human heads are very similar. This conclusion justifies designing control algorithms and performing experiments with the aid of the artificial head, and subsequent application of the results to the human head. In the case of a loose seal (the earmuff is not uniformly applied to the head and the distance reaches about 1 cm at some points) the difference increases, mainly in the gain—see Figure 2. Therefore, to achieve satisfactory performance, control algorithms should be provided with adaptation features. It can also be observed in Figure 2 that due to analogue filters, the signal can be considered as sufficiently suppressed at the Nyquist frequency, taking into account the trade-off between increasing the order of analogue filters and the demand to not introduce very large phase lags degrading control system performance.

Most of the ANC feedforward algorithms used require a plant model in the controller parameters update procedure. One of them, commonly referred to in the literature, is Filtered-x LMS (FXLMS, see Figure 4) that for FIR filter can be expressed by the following formula:

$$\hat{\mathbf{w}}(i+1) = \hat{\mathbf{w}}(i) + \mu(i) \hat{\mathbf{r}}(i) y(i), \quad \hat{\mathbf{r}}(i) = \hat{\mathbf{p}}^T \mathbf{x}(i). \quad (1)$$

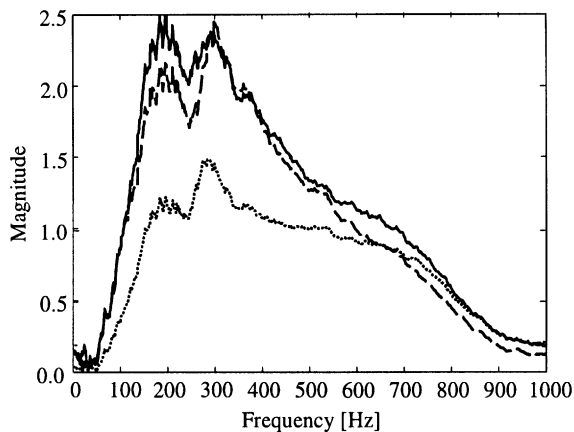


Figure 2. Magnitudes of frequency responses of the plant with different loads: ---, artificial head; —, human head (tight seal);, human head (loose seal).

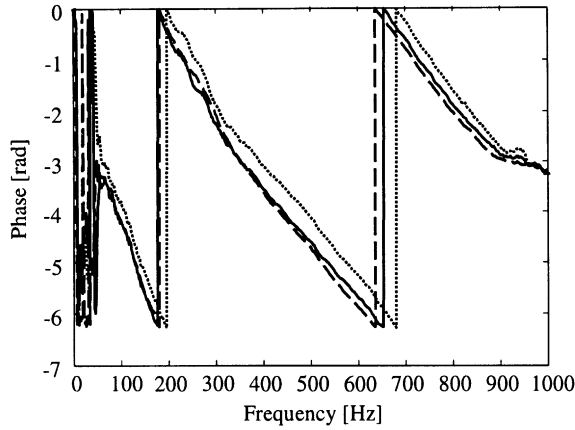


Figure 3. Phases of frequency responses of the plant with different loads: ---, artificial head; —, human head (tight seal);, human head (loose seal).

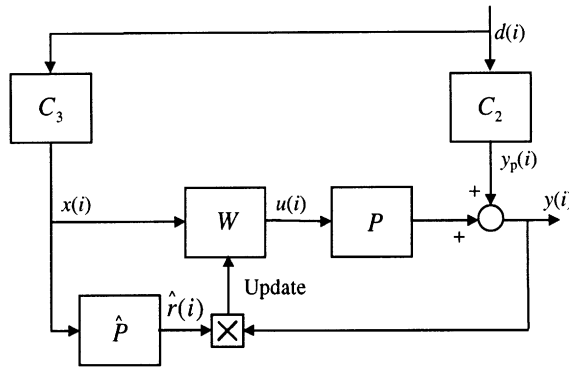


Figure 4. Feedforward control with filtration of the reference signal: C_2 , the primary path; C_3 , the reference path; P , the plant.

In equation (1), see also Figure 4, $\hat{\mathbf{w}}(i) = [\hat{w}_0(i), \hat{w}_1(i), \dots, \hat{w}_{N-1}(i)]$ is the estimate of the impulse response of the control filter $W(i)$, $\hat{\mathbf{p}}(i) = [\hat{p}_0(i), \hat{p}_1(i), \dots, \hat{p}_{N-1}(i)]$ is the estimate of the impulse response of the plant $P(i)$, $\mathbf{x}(i) = [x(i), x(i-1), \dots, x(i-N+1)]$ is the filtered input signal, $\hat{\mathbf{r}}(i) = [\hat{r}(i), \hat{r}(i-1), \dots, \hat{r}(i-N+1)]$ is the filtered reference signal, and $\mu(i)$ is the step-size. However, model-based algorithms (FXLMS or others, e.g., minimum variance [1, 7]) are exposed to errors introduced by the model. It is not always possible to adapt the model to changes in the plant while applying a control algorithm or the model may be poor due to significant bias errors [8]. Besides, rich model structures, needed for accurate plant modelling, are often not acceptable. If the model structure is large, the algorithm becomes too slow; in this case the control filter structure is also large which further slows down the algorithm. On the other hand, if the model is identified only prior to control it may be inadequate later on due to plant parameter changes, e.g., a loose seal between the earmuff and the head (in AHPD—see the characteristics in Figures 2 and 3), head movements (in active headrests), people movement (in “silent rooms”), etc. [1, 6]. Alternative robust control involves stability/attenuation trade-off that degrades the performance [1]. Other more sophisticated modifications, usually very time consuming, are applicable only to a limited group of applications.

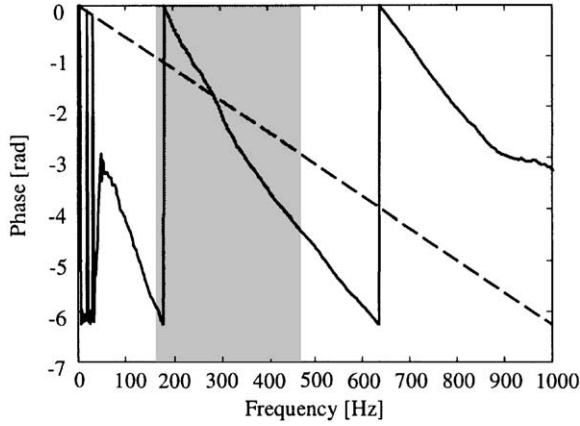


Figure 5. Phases of frequency responses of the plant and its discrete time delay (of 2 samples); —, plant; ---, plant delay; grey area, theoretical attenuation band.

In this paper, another approach is proposed. Using the so-called delayed LMS (DLMS) instead of FXLMS allows in getting rid of the full model [1, 3, 19]. This is so, because for DLMS the reference signal is not filtered by the plant model, but only delayed by its discrete time delay, k :

$$\hat{\mathbf{w}}(i+1) = \hat{\mathbf{w}}(i) + \mu(i)\mathbf{x}(i-k)y(i). \quad (2)$$

Therefore the plant estimate in Figure 4 is substituted by z^{-k} , i.e., k -step backward shift operator. According to the literature, this algorithm can converge for sine signals (tonal noises for ANC applications) if the phase mismatch between the plant and the delay is less than $\pi/2$, [10, 11]. A comparison of phase characteristic of the plant considered for experiments and a delay of 2 sampling intervals (such a delay was identified) is presented in Figure 5 [1]. On this basis it was found that attenuation could be obtained over the frequency range of 170–470 Hz (the grey rectangle in the figure). However, the best results are expected when the phase lags are comparable. To obtain satisfactory performance over a wider frequency range, for both narrowband and broadband noise, a new compound algorithm will be proposed in the following sections.

3. ACTIVE CONTROL OF NARROWBAND NOISE—A PHYSICAL APPROACH

Sine signals (electric or acoustic) passing through linear paths; C_2 , C_3 , and the plant, P (see Figure 4), are changed only in amplitude and phase. To achieve good noise attenuation at the system output, $y(i)$, it is thus sufficient to scale the reference signal in amplitude, delay it in time and drive the plant. The time delay should correspond to the phase shift $\Delta\varphi$, which satisfies the following phase equation (time delay and phase shift are equivalent):

$$\varphi_p = \varphi_r + \varphi_s + \pi + 2n\pi + \Delta\varphi, \quad (3)$$

where φ_p is the phase shift of the primary path (C_2), φ_r the phase shift of the reference path (C_3), φ_s the phase shift of the secondary path of the plant, π symbolizes delay of a sine of half its period, n the integer number and $\Delta\varphi$ the phase shift performed by the algorithm.

Such a solution is justified not only for sine signals but also for more complex narrowband signals of spectra concentrated around a fundamental frequency. This is because within a narrow frequency band both the magnitude and phase change little. Besides, for the primary and reference paths the changes are in the same direction which, according to equation (3), compensates them to some extent. Obviously, for CAPs it only refers to deterministic signals, which can be predicted well by delaying them by a number of periods. Due to the continuous character of the plant, time delays introduced by all its parts are not integer multiples of the sampling period. Therefore, to fulfil relation (3), an algorithm able to model the required phase shift has to be proposed.

3.1. PHASE SHIFTER

The operator z^{-h} is only a rough approximation of continuous-time delay required for the controller. The error of this approximation does to exceed half the sampling period. So the need for continuous delay correction corresponding to half the sampling period still exists. To obtain it, a very simple correction, $1/(1 - b(i)z^{-1})$, is sufficient [12]. A scale factor, $a(i)$, added to such a filter ensures amplitude matching of the two signals to be interfered. As the final result, the algorithm named the *Phase Shifter* (PHS) has the following form:

$$W = z^{-h} \frac{a(i)}{(1 - b(i)z^{-1})}. \quad (4)$$

Parameters $a(i)$ and $b(i)$ are updated, according to the DLMS algorithm in the version for IIR filters (see reference [9]),

$$\begin{aligned} \hat{a}(i+1) &= \hat{a}(i) + \mu(i)x(i-k-h)y(i), \\ \hat{b}(i+1) &= \hat{b}(i) + \mu(i)u(i-k-1)y(i), \end{aligned} \quad (5)$$

where k is the discrete plant delay required in DLMS (see (2) and Figure 5). The value of control, being the reference signal processed by the control filter:

$$u(i) = \frac{a(i)}{(1 - b(i)z^{-1})} x(i-h), \quad (6)$$

is calculated according to the simple recursion:

$$u(i) = a(i)x(i-h) + b(i)u(i-1). \quad (7)$$

From equations (4) and (7) it follows that the phase shifter is a special case of low order IIR filter (and therefore it inherits features of such filters [9, 12], but with only three parameters (h , $a(i)$, $b(i)$) to be estimated. Nevertheless, contrary to conventional IIR filter, one of the estimated parameters is the discrete time delay that for some plants, other than CPAs, can be significantly large.

In order to achieve good attenuation effects, it is imperative to reverse the phase of the signal (shift it by π). Therefore for signals of various frequencies, various discrete time delays may be needed and a proper estimation of h is essential. Assuming temporarily constant time delays introduced by the primary ($\varphi_p = \text{const}$), reference ($\varphi_r = \text{const}$), and secondary ($\varphi_s = \text{const}$) paths, the discrete time delay, h , depends only upon the frequency of the signal

TABLE 1

Evaluated discrete time delays, h, of PHS for some tones

h	1	2	3	4	5	6	7	8	9	10
f (Hz)	550	350	300	500	400	300	400	350	400	450
		400		550	500	500		500		500
		500				550				

(primary noise) being considered. Its value is suggested to be evaluated generally, as described below. Successive numbers are taken as h (up to the arbitrary chosen upper limit, e.g., $h_{Max} = 10$). Then, the DLMS estimation algorithm is started for a limited discrete time. This time is the number of samples equal to h_{Max} times an assumed number of samples T (e.g., 200 samples) used to calculate a quality rating, \mathfrak{I}_h , for each h plus T first samples (omitted in calculations) required for the transient stage. Thus, the quality rating, generally expressed as

$$\mathfrak{I}_h = \sum_{l=1}^T y^2(hT + l), \quad (8)$$

is calculated. Then h is assumed to be equal to that value for which \mathfrak{I}_h is minimal. Discrete time delays for various signals, estimated in real-world experiments are shown in Table 1. It should be noted that the assignment of values of h to frequency values is not unique, which is both theoretically and intuitively obvious. Besides, if the primary noise changes, h may be also subject to change. Changes of $\varphi_p, \varphi_r, \varphi_s$, are corrected by $b(i)$ in the adaptive process as they usually do not rather involve correction of the discrete time delay (see Figures 2 and 3, even for the loose earmuff seal).

3.2. PHASE SHIFTER-2

Phase Shifter-2 algorithm (PHS2) is based on a similar concept as PHS. The number 2 in its notation comes from *two* parameters to be estimated:

$$W = z^{-v} \frac{g(i)(c(i) + z^{-1})}{(1 + c(i)z^{-1})}. \quad (9)$$

The discrete time delay, v , contrary to h for PHS, can be easily found prior to experiments because it is not dependent on the noise frequency (for the APHPD considered it was $v = 1$). This is due to the fact that parameter $c(i)$ assures phase matching over the range $\langle -\pi, 0 \rangle$. The magnitude of frequency response of the control filter is uniform and equal to $g(i)$. It is advantageous that only two parameters are to be estimated and the filter meets all the requirements for active control of any tonal (or more complex narrowband) noise. The adaptation procedure can be derived on the basis of equation (9) and the fact that control signal is calculated as the reference signal processed by the control filter. Thus,

$$u(i) = \frac{g(i)(c(i) + z^{-1})}{(1 + c(i)z^{-1})} x(i - v). \quad (10)$$

Then, according to the DLMS algorithm in the version for IIR filters (see reference 9), the update equations take the form

$$\begin{aligned}\hat{g}(i+1)\hat{c}(i+1) &= \hat{g}(i)\hat{c}(i) + \mu(i)x(i-k-v)y(i), \\ \hat{c}(i+1) &= \hat{c}(i) + \mu(i)u(i-k-1)y(i),\end{aligned}\quad (11)$$

where k is the discrete plant delay required in DLMS (see equation (2) and Figure 5). Making substitutions

$$\hat{g}(i)\hat{c}(i) = \hat{w}_0(i) \quad \hat{g}(i) = \hat{w}_1(i), \quad (12)$$

gives a more coherent form

$$\begin{aligned}\hat{w}_0(i+1) &= \hat{w}_0(i) + \mu(i)x(i-k-v)y(i), \\ \hat{w}_1(i+1) &= \hat{w}_1(i) + \mu(i)u(i-k-1)y(i).\end{aligned}\quad (13)$$

The example results are presented in Table 2.

Combining equations (10) and (12), the control law takes the form

$$u(i+1) = \hat{w}_0(i+1)x(i-v+1) + \hat{w}_1(i+1)x(i-v) - \frac{\hat{w}_0(i+1)}{\hat{w}_1(i+1)}u(i), \quad (14)$$

Performance features of PHS2 are very similar to features of PHS. However, it does not need estimation of discrete time delay, v , which takes a major part of the entire computation time. Concluding, PHS2 algorithm seems to be better than PHS. But on the other hand, in PHS2 only one parameter, $c(i)$, is responsible for phase correction by π while in PHS algorithm, parameter $b(i)$ adjusts the phase only by $(f/f_s)\pi$ (e.g., for $f = 400$ Hz and $f_s = 2000$ Hz, the adjustment is by $\frac{1}{5}\pi$). So the sensitivity of PHS2 is very high (at least four times higher than that of PHS) and therefore its robustness to non-stationarities is poorer. Again, PHS2 is an IIR filter and therefore it inherits features of such groups of filters 9.

3.3. EXPERIMENTAL RESULTS

A comparison of attenuation results, J_{band} (measured in the band from 0 to 5000 Hz, to take into account effects of plant non-linearity and inter-sample behaviour [1]), obtained by PHS, PHS2, FIR and IIR filters identified via DLMS is presented in Figure 6. The signals used for experiments were pure tones. However, due to some non-linear effects as well as the acoustic background and other, e.g., measurement noises, their spectra were richer. Attenuation of fundamental frequencies, J_1 , is about 60 dB. To achieve comparable

TABLE 2

Estimated parameters, c and g , of PHS2 for some tones

f (Hz)	300	350	400	450	500
c	-0.322	0.408	0.278	0.445	0.624
g	0.846	0.804	0.987	1.033	1.081

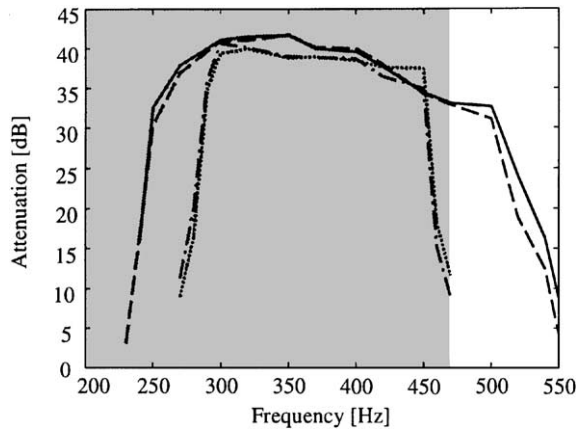


Figure 6. Attenuation results, J_{bands} of PHS, PHS2, FIR(31) and IIR (9, 10) adaptive filters estimated via DLMS (the numbers of estimated parameters are given in parentheses): —, PHS; ---, PHS2; - · - · -, FIR; ····, IIR.

values of attenuation, different numbers of parameters, depending on the algorithm applied, are required. For FIR filter at least 31 parameters are to be estimated, for IIR—no less than 19, while for PHS—3, and for PHS2—2. Moreover, the phase shifters managed to attenuate signals in essentially wider (over 100 Hz) bands than the other algorithms. As it is seen, the attenuation bands differ slightly from those determined in theoretical analysis. This difference may result from the presence of other noises, not taken into account in the theoretical analysis as well as from non-stationary effects that change phase characteristics of the plant. Figure 7 presents exemplary attenuation results of noise with dominant tone of frequency 300 Hz. Second and third harmonics as well as some background noise can also be observed well. It is worth noticing that signal components of frequencies lying beyond the band depicted in Figure 6, e.g., those harmonics from Figure 7 are not attenuated. However, in this experiment the system remains stable, particularly because the harmonics and background noise are on much lower levels than the dominant tone. Nevertheless, in general, the presence of broadband noise or other deterministic components in significant levels may lead to divergence of the adaptive filter parameters and instability of the entire system. To protect against this effect, algorithms using a simplified plant model should be supported by fixed band-pass filters that limit spectrum width of the signal, before it is adaptively filtered. This approach is further explained in the following sections.

Concluding, the proposed phase shifters exhibit the following features:

- their concept is based on a physical approach to noise control problems;
- they are suitable for narrowband (deterministic for CAPs) noises with spectra concentrated around fundamental frequencies. However, they can be easily extended to any noises, as shown in the next sections;
- with a minimal number of parameters—an order less than for FIR and IIR filters—they guarantee comparable attenuation;
- they give an extended attenuation band: $\langle 240; 550 \rangle$ Hz (when identified by DLMS);
- they constitute wide-band filters;
- their convergence speed is very fast and independent of the noise spectrum. For sampling with 2 kHz the adaptation time is much shorter than 0.1 s, while for the conventional FIR and IIR filters used this time exceeds 0.6 s and changes with the noise frequency;

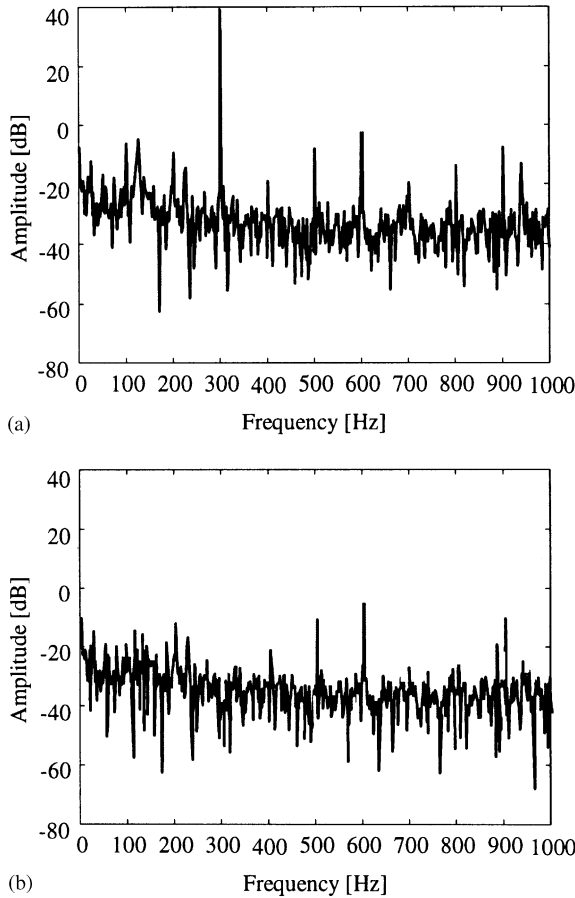


Figure 7. Noise with dominating tone of frequency 300 Hz—before (a) and after (b) cancellation.

- being in fact IIR filters, they accumulate quantization errors (but much less than high order IIR conventional filters required to yield comparable performance);
- they cope perfectly with damped tonal primary noises and with their fast frequency changes up to 30 Hz (for FIR filters it was about 50 Hz, but for IIR filters—5 Hz).

4. ACTIVE CONTROL OF BROADBAND NOISE

According to the previous section, phase shifters converge very fast and therefore immediately, without annoying the user, track any non-stationarities of the plant or noise. This is a direct consequence of the simplified plant model used, which allows for updating only a few parameters in the entire adaptive algorithm. However, phase shifters, in the forms presented so far, have only limited applications. They are able to attenuate exclusively individual tones of frequencies inside the attenuation band, or complex narrowband (deterministic for CAPs) noises with spectra concentrated around fundamental frequencies in this band. Other noises appearing, depending on their levels, may lead to divergence of estimated parameters. Below, the idea of phase shifters will be extended to broadband noises.

4.1. PHASE SHIFTER BANKS

Phases shifters are proposed to be connected in parallel channels referred to as banks. Hence, this extension is named *PHS-Banks*. Each bank consists of a band-pass filter and a PHS (alternatively PHS2), see Figure 8. Experiments showed that a PHS can cope well with a signal having spectrum not wider than about 40 Hz (± 20 Hz around the fundamental frequency). Therefore, each filter should be properly designed to pass through an individual bank signal of proper spectrum. Particular care must be taken not to allow magnitudes of frequency responses of neighbouring filters to overlap resonance peaks (see Figure 9 for example filters). As a consequence, each filter has to have a sufficiently high selectivity. Very low selectivity generates signal components in neighbouring banks with irrelevant spectra and significant levels. This can lead to poorer attenuation results or even to parameter divergence in the bank. To increase selectivity the filter order has to be increased. However, under the above constraints, the described algorithm is able to attenuate any noise in the whole band covered by all the PHS filters taken together.

It is important that all the PHS filters are used for bands known beforehand. Thus, their discrete time delays, h_1, \dots, h_n , can be fixed in advance and do not have to be estimated. Summarizing, for n banks only $2n$ parameters: $a_1(i), \dots, a_n(i)$, and $b_1(i), \dots, b_n(i)$ require estimation (by DLMS); this is the same number of parameters as for PHS2. However, it is still possible to estimate the discrete time delays using the quality rating, \mathcal{T}_h (see equation (8)). In this case, the error signal, $y(i)$, used in update procedures of the adaptive filters should also be shaped in each bank by a relevant band-pass filter (F_1-F_n). It is not always necessary to process the noise in each bank because respective frequency components may be absent. Therefore, it is recommended to compare maximal values of filtered signals, $x_1(i)$ to $x_n(i)$, with threshold values assumed beforehand and not to employ banks which are targeted at frequencies that are not in the signal (noise). An important feature of this algorithm having a great practical meaning is that it allows cancelling of only selected narrowband signals or passing only selected narrowband signals. This permits, contrary to most noise control designs met in the literature, speech communication and hearing warning sounds.

4.2. EXPERIMENTAL RESULTS

For presentation, in the real-world experiments four banks were implemented. IIR(10, 10) filters were employed as F_1-F_4 (see Figure 8). They were designed using the least-squares method. These filters were adjusted to frequencies: 350, 400, 450, and 500 Hz (see Figure 9).

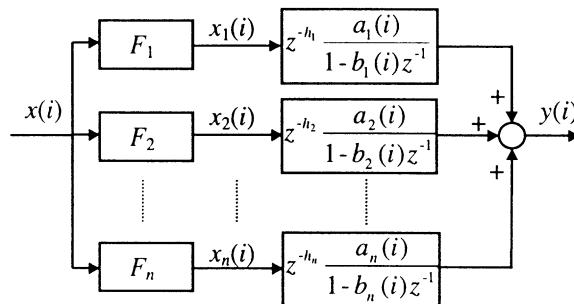


Figure 8. Block diagram of PHS-Banks algorithm.

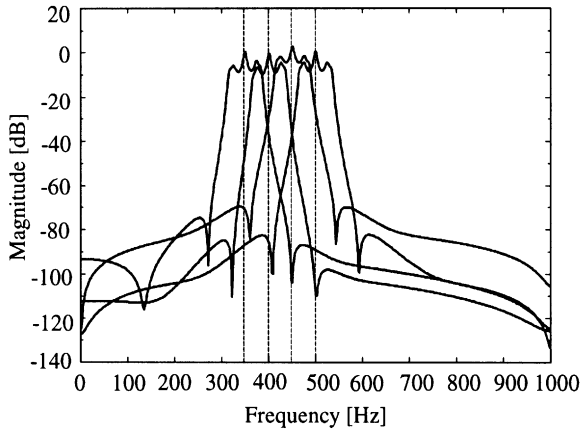


Figure 9. Magnitudes of frequency responses of four filters designed for PHS-Banks.

As the signal for experiments, multitonal noise consisting of four tones of those frequencies and some background noise were generated (see Figure 10). Harmonics of the tones also appeared. Attenuation of the fundamental frequencies, J_1 , was over 50 dB for each individual tone generated, but measured in the band, J_{band} , for the overall noise—over 30 dB. The harmonics and the background noise are not attenuated, as the control algorithm, due to the presence of selective filters F_1 – F_4 , does not process them. It must be emphasized here that the adaptation time has been increased to about 0.1 s due to the processing of the signal by the selective filters. However, the conventional FIR and IIR filters used in this article for comparison required more than 1 s.

5. EXTENSION OF THE ATTENUATION BAND

Experiments performed with various sampling frequencies (2, 1, 0.5 kHz) and feedforward control using phase shifters show that for each sampling frequency, the attenuation bands are adjacent or slightly overlapping and approximately octave. They can be summarized as follows: $f_s = 2 \text{ kHz} \Rightarrow f \in \langle 240; 550 \rangle \text{ Hz}$; $f_s = 1 \text{ kHz} \Rightarrow f \in \langle 140; 310 \rangle \text{ Hz}$; $f_s = 0.5 \text{ kHz} \Rightarrow f \in \langle 100; 140 \rangle \text{ Hz}$ [13]. On the basis of these results (Figure 11) it was found that by varying the sampling rate, it is possible to move noise attenuation bands along the frequency axis and their octave character is almost maintained (for $f_s = 0.5 \text{ kHz}$ the lower limit is imposed by the pass-band of the loudspeakers used and plant non-linearity). Similar behaviour was noticed for other filters identified via DLMS, i.e., using the simplified plant model.

5.1. THE IDEA OF MULTIRATE SIGNAL PROCESSING

An algorithm converting a signal sampled with some arbitrary frequency to signals as if they were sampled with other frequencies, and processing them is termed *multirate signal processing* (MSP) [12]. This algorithm is illustrated in Figure 12. It consists of the following blocks:

- band-pass (low-pass in classical MSP) discrete anti-aliasing filters (F_{D2} , F_{D3});
- down-samplers ($\downarrow D$);

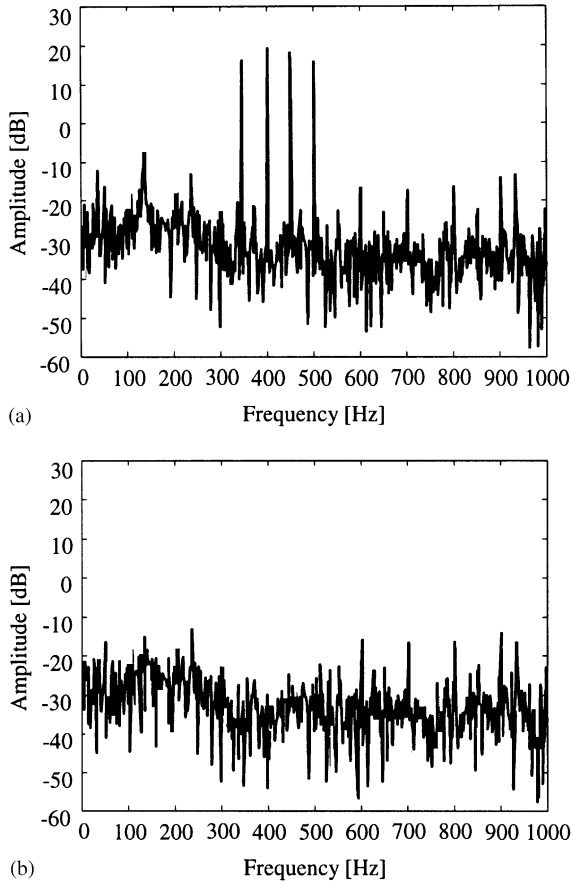


Figure 10. Multitone noise consisting of frequency components: 350, 400, 450 and 500 Hz, and background noise.

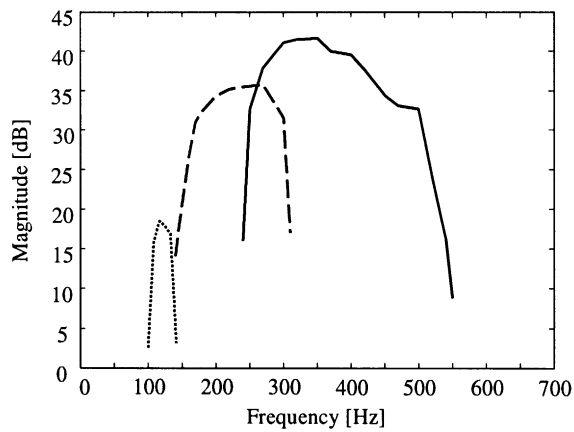


Figure 11. Attenuation results for PHS with different sampling frequencies: —, $f_s = 2$ kHz; ---, $f_s = 1$ kHz; $f_s = 500$ Hz.

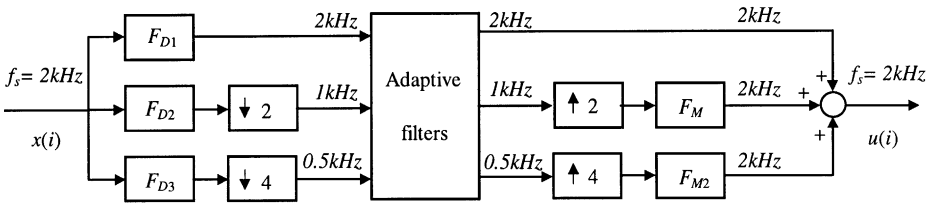


Figure 12. MSP structure.

- adaptive filters;
- up-samplers ($\uparrow M$);
- low-pass discrete anti-imaging filters (F_{M1}, F_{M2}).

The process of decreasing D -times the sampling rate of a signal is referred to as decimation by D . It consists in removing $D-1$ samples between neighbouring samples (down-sampling). This can cause the so-called aliasing error and to avoid it, an anti-aliasing discrete filter (that has nothing to do with the anti-aliasing analogue filter in Figure 1) with pass-band maximal frequency less than $f_s/2D$ has to be first used (F_{D2}, F_{D3} in Figure 12; F_{D1} is only to select the signal components that should be processed with the original sampling frequency). Analogously, the process of increasing M -times the sampling rate of a signal is referred to as interpolation by M . It consist in inserting $(M - 1)$ zeros between existing neighbouring samples (up-sampling). This can cause the so-called imaging effect and to avoid it, an anti-imaging discrete filter with pass-band maximal frequency less than or equal to $f_s/2M$ has to be used as the next block (F_{M1} and F_{M2} in Figure 12).

In view of the problem being discussed, noise measured by the reference microphone is sampled with a rate of 2 kHz and then passes concurrently through three channels. Each one processes a part of the signal, having spectrum in one of the bands depicted in Figure 11. This is ensured by band-pass filters: F_{D1}, F_{D2}, F_{D3} . The last two filters play the role of anti-aliasing discrete filters, as well. In the sequel, sampling rate is converted in two of the channels, and three obtained signals (with sampling rates of 2, 1, and 0.5 kHz, respectively) are adaptively filtered by phase shifters. Finally, sampling rates are established in all the channels on 2 kHz by interpolation procedure in two of them and a common control signal is sent to the plant.

5.2. DIGITAL FILTERS DESIGN CONSIDERATION AND COMPUTATIONAL LOAD ANALYSIS

While designing an MSP system there are many degrees of freedom. Traditionally, low-pass filters are used as the anti-aliasing discrete filters (in classical MSP). Among different possible filters, FIR filters designed to have symmetrical parameters and consequently linear phases over the whole frequency range are recommended. Their impulse responses, θ , for odd number of parameters, N_2 and cut-off frequency being $f_s/2D$, satisfy

$$\theta_{((N+1)/2+j)} = 0, \quad j = \pm lD, \quad l < \frac{N}{2D}. \quad (15)$$

Additionally, if a ladder structure is used, the required number of multiplications, κ , is reduced to

$$\kappa = \frac{(N+1)}{2} - \text{trunc} \left(\frac{N}{2D} \right), \quad (16)$$

where $\text{trunc}(N/2D)$ denotes the closest but not greater than $N/2D$ integer value. The number of parameters depends on requirements concerning transmission-band of a filter. If any so-called “do not care bands” are permissible, then N can be adequately decreased.

The design of anti-imaging discrete filters is similar with D replaced by M in equations (15) and (16). In the case of low-pass filters with cut-off frequencies being $f_s/2M$ and if additionally M can be factorable into a product of j integers, $M = M_1 M_2 \dots M_j$, it is often more efficient to perform multistage sampling rate conversion. For instance, for $M = 4$, $N = 17$ and one-stage procedure, according to formula (16), 7 multiplications are needed. In turn, to obtain the same spectral features for two-stage conversion only $N = 9$ parameters per stage are required which leads to $\kappa = 6$.

Adaptive control filters in the multirate ANC system can be (and should be) adjusted to control noise in adjacent, approximately octave bands lying in the middle of frequency ranges limited by respective Nyquist frequencies as Figure 11 shows. Then band-pass octave filters as anti-aliasing filters are strongly recommended (F_{D1} , F_{D2} , and F_{D3} in Figure 11). Such filters being properly designed can have most of their parameters identically equal to zero and symmetrically distributed [13]. For example, for $N = 17$ parameters only 4 multiplications are required. Moreover, these filters have linear phases. Sometimes, despite numerical optimization, the computational load is still too high. This usually takes place when the sampling rate is relatively high and the algorithm (like noise control procedure) has high complexity. Then, some approximations can be used. The most time-consuming part in sampling rate conversion is the interpolation procedure (or rather anti-imaging filtering—filters F_{M1} , F_{M2}). Interpolation can be substituted by *zero order hold (ZOH)*—see Figure 13. Samples worked out by adaptive filter with 1 kHz are held for unit discrete time (ZOH_{1s})—referred to $f_s = 2$ kHz—and those worked out with 0.5 kHz are held for three discrete time delays (ZOH_{3s}). All of the three channels contribute to the common signal sent to the plant. This solution loses negligibly little information, protects the signal against imaging effect and involves no multiplications, thereby significantly reducing the computational time.

If required, MSP makes noise attenuation over a much wider frequency range than presented in Figure 11 possible by adding other channels and sampling with a higher frequency. The practical limitations are only due to the efficiency of the signal processor used.

5.3. COMBINING MSP AND PHS-BANKS

It is also possible to combine PHS-Banks with MSP to obtain wide-band attenuation of broadband noises. In the era of rapid development of microelectronics, even such a quite sophisticated algorithm is feasible. It constitutes a combined non-parametric and parametric approach to control, which is rather rarely met in control system literature. In this algorithm the anti-aliasing digital filters, F_D , used in the decimation procedure (see Figure 12) are not necessary because relevant band-pass filters designed for each bank (see Figure 8) do not allow passing frequency components above $f_s/2D$.

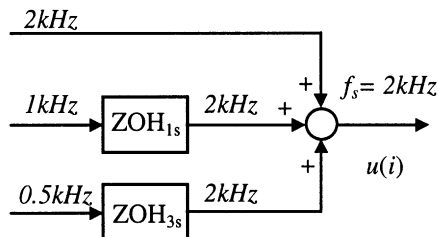


Figure 13. Interpolation with ZOHs.

Block diagram of the algorithm designed and implemented within this work is depicted in Figure 14. For presentation, six banks are considered. The first three banks are designed to attenuate three tones in the first channel with the original sampling frequency of 2 kHz. Next, two banks are set to attenuate two tones in the second channel with a sampling frequency of 1 kHz. The last bank aims at attenuating a tone in the third channel with sampling frequency of 500 Hz. Each filter F_{pq} is designed to selectively pass respective q th frequency, guaranteeing, by the way, anti-aliasing filtration in p th sampling conversion channel. The signal components represent the three bands noted in Figure 11. Therefore, in two channels, after filtering the signal measured with 2 kHz, the sampling frequency is reduced to 1 kHz and 500 Hz. Being protected against aliasing, this is performed by simply removing, respectively, one and two samples between neighbouring samples. Next, all signal components are filtered by phase shifters. Each phase shifter, responsible for individual bank, requires adaptation of two parameters, which is done with DLMS algorithm. Signal components operating with the same sampling frequency are then summed. In two channels, sampling conversion is performed to return to 2 kHz. The time-consuming classical interpolation procedure is substituted with ZOHs by holding samples for one and three discrete time delays respectively. Finally, outputs of all the channels contribute to the control signal driving the plant.

A similar system could also be designed, in which the order of isolating the frequency components in filters F_{pq} and down-sampling was changed—see Figure 15. However, in this approach additional discrete anti-aliasing filters are necessary. In turn, the advantage is that for all banks operating with the same reduced sampling rate, down-sampling is performed only once. Nevertheless, taking into account the fact that down-sampling is simply omitting some samples, this advantage is only merely apparent. Concluding, the second approach presented involves more calculations which increases computational load without improving the performance of the cancellation algorithm. Therefore, results of the experiments presented below are obtained with the structure depicted in Figure 14.

5.4. EXPERIMENTAL RESULTS

The signal used for experiments was multitonal noise of frequency components 120, 200, 250, 350, 400, 450 Hz matching settings of the F_{pq} filters in Figure 14. Additionally, it contained tones of frequencies 80, 600, 700 Hz, some background noise, as well as

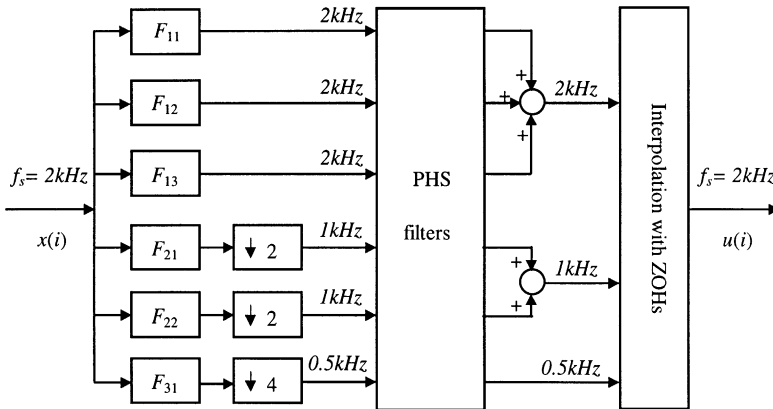


Figure 14. Combination of MSP and PHS-Banks.

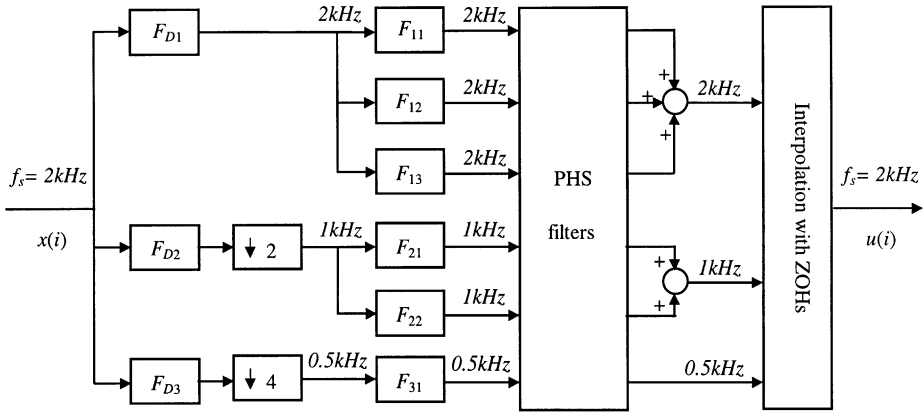


Figure 15. Combination of MSP and PHS-Banks—an alternative structure.

harmonics generated due to non-linear effects, to check stability and selectivity of the entire system. As it is seen from Figure 16, the frequency components allowed for processing, by filters in banks, are well attenuated with J_{band} exceeding 30 dB (J_1 reaches over 50 dB for some tones). Other tones as well as the harmonics generated are passed “untouched”. It is important to note that the entire system remains stable even if the signal is of substantially richer spectrum. Convergence rate of the overall algorithm is very high. After starting it takes about 0.2 s to reach the “steady state”. Then, all the filters adapt to non-stationarities introduced into the system (by moving the head fast, loosening the earmuff seal or changing noise level) in a time shorter than 0.1 s.

For comparison, similar experiments were performed with conventional filters. However, to cover such a wide spectrum of the signal generated, they required FXLMS instead of DLMS algorithm. This in turn, involved accurate wide-band plant modelling. To obtain high attenuation (still much worse than for the algorithm proposed), the plant was modelled with 128 parameters of FIR filter. Control filters had the following structures: for FIR filter—128, and for IIR filter—32 coefficients. For such a parameterization, the convergence time was more than 3 s, which cannot be accepted for many applications, e.g., AHPDs. It should also be mentioned that to obtain better attenuation, both the plant model and control filters would require larger structures, which further increases the adaptation time.

6. CONCLUSIONS

In this paper, adaptive feedforward control of acoustic noise has been discussed. Conventional algorithms, to maintain stability and provide reasonable attenuation, require many coefficients of both the plant model as well as the control filter that need to be updated sequentially. This significantly reduces the speed of convergence, which is not acceptable for some applications. Besides, it is difficult to freely shape the attenuation band. In this work, no plant model except its delay has been used. This resulted in employment of DLMS instead of FXLMS for estimation of control filter parameters. According to the literature, such a simplification imposes strong constraints on width and localization of the primary noise spectrum in order to avoid divergence of estimated controller parameters. The drawback of attenuating only narrowband noise has been turned to advantage. Because plant response changes little over the narrow frequency range the number of estimated controller parameters has been reduced to barely two. Two controllers (two

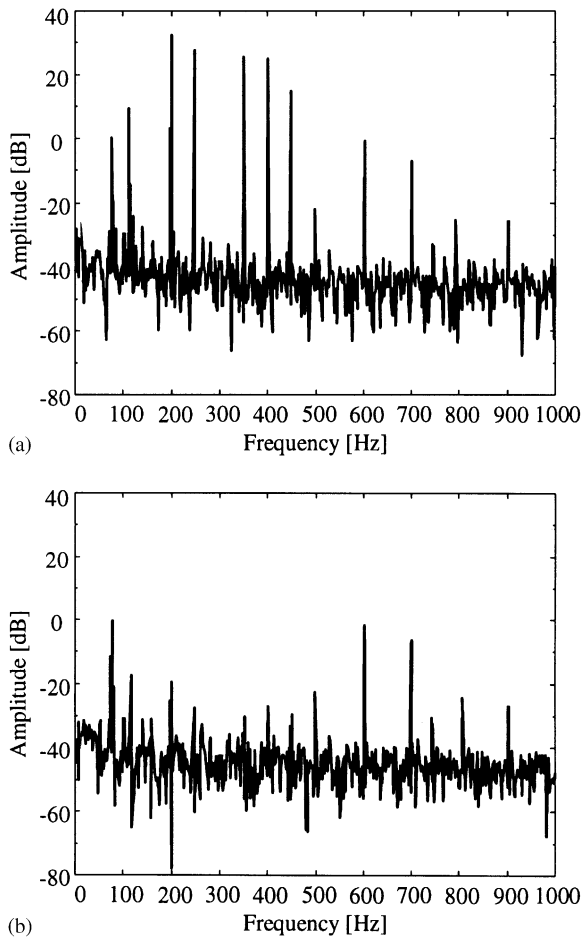


Figure 16. Multitonal noise consisting of frequency components: 80, 120, 200, 250, 350, 400, 450, 600 and 700 Hz, and background noise—before (a) and after (b) cancellation.

versions of phase shifters) have thus been proposed and examined. In addition to significant reduction of the number of required parameters, these controllers give globally much better results than other classical FIR or IIR filters, as they are set for dedicated narrow bands. To extend the field of applications of the adaptive controllers proposed, two further concepts have been put forward and analyzed. The first consists in connecting phase shifters in banks to control complex noises. The second consists in adopting multirate signal processing to widen the attenuation band. The compound algorithm combining phase shifter banks with multirate signal processing allows in controlling broadband noise over a very wide frequency range also guaranteeing the stability of the entire system. It should be noted that although this algorithm seems to be complicated and for complex noises may require estimation of many coefficients, the coefficients are adapted in parallel banks and therefore the process does not differ generally from updating only two parameters of one filter, thereby providing very fast adaptation which taken together with high attenuation is essential for the user.

As the exemplary plant for experiments, an active personal hearing protection device has been chosen. It is an example of compact acoustic plants. Due to geometrical constraints in

such plants, feedforward control makes practical sense only for deterministic noises. Therefore, multitonal noise with some acoustic background has been used. The obtained results have confirmed the expectations. The attenuation reaches at least 30 dB (for J_{band}) over the frequency range from 100 to 550 Hz with a very high speed of convergence (the adaptation to changes in the plant or noise takes about 0.1 s), providing great comfort to the user. The upper bound was imposed only by the speed of the signal processor employed, and the lower bound was limited by the pass-band of the secondary source. Due to filtration in banks, signal components of richer spectrum are not attenuated but they also do not influence the stability of the entire system.

Some other features of the algorithm proposed also deserve to be mentioned. It is able to effectively control random noise in plants not belonging to the CAP group. Besides, if necessary, it allows the control of only selected bands and freely passing others, e.g., bearing warning or alarming information.

REFERENCES

1. M. PAWELCZYK 1999 *Active Noise Control for Compact Acoustic Plants*. Gliwice: Jacek Skalmierski Computer Studio.
2. P. A. NELSON and S. J. ELLIOTT 1994 *Active Control of Sound*. Cambridge: Academic Press Limited.
3. C. HANSEN and S. D. SNYDER 1997 *Active Control of Noise and Vibration*. Cambridge: E & FN Spon, an imprint of Chapman & Hall, Cambridge University Press.
4. M. WINBERG, S. JOHANNANSSON, T. LAGÖ, I. CLAESSION 1999 *International Journal of Acoustics and Vibration* **4**, 51–58. A new passive/active hybrid headset for a helicopter application.
5. G. B. B. CHAPLIN, R. A. SMITH and T. P. C. BRAMER 1987 *US Patent* 4,654,871. Method and apparatus for reducing repetitive noise entering the ear.
6. B. RAFAELY 1997 *Ph.D. Thesis, Institute of Sound and Vibration Research, University of Southampton, Feedback control of sound. Southampton*.
7. M. PAWELCZYK, S. J. ELLIOTT and B. RAFAELY 1997 *Southampton University, Institute of Sound and Vibration Research Technical Memorandum No. 822*. Active noise control using feedback. Fixed and adaptive controllers.
8. B. RAFAELY, S. J. ELLIOTT 1996 *Southampton University, Institute of Sound and Vibration Research Technical Memorandum No. 776*. Internal model controller for feedback control of sound and vibration.
9. S. M. KUO, D. R. MORGAN 1996 *Active Noise Control Systems. Algorithms and DSP Implementations*. New York: J. Wiley & Sons.
10. R. M. MORGAN 1980 *IEEE Transactions on Acoustics, Speed and Signal Processing* **28**, 454–467. An analysis of multiple correlation cancellation loops with a filter in the auxiliary path.
11. J. C. BURGESS 1981 *Journal of Acoustical Society of America* **70**, 715–726. Active adaptive sound control in a duct: a computer simulation.
12. S. K. MITRA, J. K. KAISER 1993 *Handbook for Digital Signal Processing*. New York: J. Wiley & Sons.
13. M. PAWELCZYK 1996 *Proceedings of the 3rd International Symposium on Methods and Models in Automation and Robotics*, Vol. 1, 111–114. Międzyzdroje, Poland: Szczecin Technical University. Multirate signal processing for broadband noise cancellation in active ear defender.